# Spatial anisotropy of the Kondo screening cloud in a type-II Weyl semimetal

Lu-Ji Wang,[1] Xing-Tai Hu,[1] Lin Li,[2] Dong-Hui Xu,[3] Jin-Hua Sun,[1,*] and Wei-Qiang Chen[4,5,†]

[1]*Department of Physics, Ningbo University, Ningbo 315211, China*

[2]*College of Physics and Electronic Engineering, and Center for Computational Sciences, Sichuan Normal University, Chengdu 610068, China*

[3]*Department of Physics, Hubei University, Wuhan 430062, China*

[4]*Shenzhen Institute for Quantum Science and Engineering and Department of Physics, Southern University of Science and Technology, Shenzhen 518055, China*

[5]*Center for Quantum Computing, Peng Cheng Laboratory, Shenzhen 518055, China*

(Received 10 April 2019; revised manuscript received 22 May 2019; published 4 June 2019)

We theoretically study the Kondo screening of a spin-1/2 magnetic impurity in the bulk of a type-II Weyl semimetal (WSM) by use of the variational wave-function method. We consider a type-II WSM model with two Weyl nodes located on the $k_z$ axis, and the tilting of the Weyl cones are along the $k_x$ direction. Due to coexisting electron and hole pockets, the density of states at the Fermi energy becomes finite, leading to a significant enhancement of the Kondo effect. Consequently, the magnetic impurity and the conduction electrons always form a bound state; this behavior is distinct from that in type-I WSMs, where the bound state is only formed when the hybridization exceeds a critical value. Meanwhile, the spin-orbit coupling and unique geometry of the Fermi surface lead to a strongly anisotropic Kondo screening cloud in coordinate space. The tilting terms break the rotational symmetry of the type-II WSM about the $k_z$ axis, but the system remains invariant under a combined transformation $\mathcal{T}R^y(\pi)$, where $\mathcal{T}$ is the time-reversal operation and $R^y(\pi)$ is the rotation about the $y$ axis by $\pi$. Largely modified diagonal and off-diagonal components of the spin-spin correlation function on three principal planes reflect this change in band symmetry. Most saliently, on the $x$-$z$ plane, tilting terms trigger the emergence of nonzero off-diagonal spin-spin correlation function $J_{yz}(\mathbf{r})$ and $J_{xy}(\mathbf{r})$, while in a type-I WSM they vanish on the $x$-$z$ plane.

DOI: 10.1103/PhysRevB.99.235108

## I. INTRODUCTION

As representatives of a new state of topological quantum matter, topological semimetals [1] which host Dirac or Weyl fermions as low-energy excitations in the bulk have attracted much attention in recent years. Three-dimensional (3D) Dirac semimetals have been realized experimentally in $Na_3Bi$ [2] and $Cd_3As_2$ [3,4] materials, where the Dirac points are stabilized by the inversion ($\mathcal{P}$), time-reversal ($\mathcal{T}$), and crystalline symmetries. If the $\mathcal{P}$ and/or $\mathcal{T}$ symmetry is broken, a transition towards the Weyl semimetal (WSM) phase takes place and each Dirac point splits into a pair of Weyl nodes [5–7]. There has been tremendous interest in WSMs because a new TaAs family of WSMs was predicted theoretically [8,9] and subsequently observed in experiments [10–17]. The Weyl fermions in the TaAs family approximately respect the Lorentz symmetry. However, the Weyl fermions realized in condensed matter physics are quasiparticles which can violate the Lorentz invariance, indicating that the Weyl cones in momentum space can be tilted.

Two-dimensional (2D) tilted anisotropic Dirac cones have been found in the 8-*pmmn* borophene [18] and in the organic semiconductor $\alpha$-(BEDT-TTF)$_2$I$_3$ [19,20]. In 3D systems, the band crossing points are more robust and generic than in 2D materials. Type-II Dirac or Weyl fermions [21–23] are obtained when Dirac or Weyl cones are tilted strongly in momentum space. In this case the electron and hole pockets coexist with the Dirac or Weyl nodes. Type-II Weyl fermions are predicted and soon confirmed in $WTe_2$ and $MoTe_2$ [22,24–28]. Very strongly robust type-II Weyl nodes are predicted in $Ta_3S_2$ [29] and observed in crystalline solid LaAlGe [30]. Type-II WSMs show remarkable properties such as an anisotropic chiral anomaly [22], unusual thermodynamic and optical responses in the presence of magnetic fields [31–34], and an anomalous Hall effect [35,36].

The Kondo effect [37] takes place when a magnetic impurity forms a singlet with the conduction electrons at a temperature lower than the Kondo temperature. In type-I Dirac or Weyl semimetals, the density of states (DOS) vanishes when the Fermi level lies at the Dirac points or Weyl nodes. Consequently, the magnetic impurity problem in these systems falls into the category of the pseudogap Kondo problem [38–40], in which a threshold of hybridization exists for the impurity and conduction electrons to form a bound state. It has been shown that the Kondo effect can be enhanced by tuning the chemical potential away from the Weyl node, and the charge imbalance between two Weyl cones with different chiralities can be detected through the magnetic susceptibility [41].

Major differences between type-I and type-II WSMs in Kondo screening originate from the band structure and the

*sunjinhua@nbu.edu.cn

†chenwq@sustc.edu.cn

 

Fermi surface of the host materials. By tuning the tilting terms in the model Hamiltonian, we are able switch the system between type-I and type-II WSM phases to compare the differences. In a type-II WSM, due to coexisting electron and hole pockets at the Fermi level, the DOS becomes finite [34]. Our results on the binding energy of a magnetic impurity embedded in the bulk of a WSM reflect this change. We find that due to the finite DOS, the bound state is always favored in the type-II WSM, whereas in a type-I WSM, in which the DOS vanishes at half-filling, the hybridization strength has a lower bound to form a bound state [42]. In addition to this, the tilting terms change the symmetry properties of the WSM, which can be shown by the spatial spin-spin correlations between a magnetic impurity and the conduction electrons. Specifically in the present paper, the tilting terms break the rotational symmetry of the WSM, leading to very interesting features such as the emergence of nonzero off-diagonal correlation functions [$J_{yz}(\mathbf{r})$ and $J_{xy}(\mathbf{r})$] on the $x$-$z$ plane. However, if the tilting terms vanish, which corresponds to the case of a type-I WSM, $J_{yz}(\mathbf{r})$ and $J_{xy}(\mathbf{r})$ are always 0 on the $x$-$z$ plane.

In this paper, we use the variational wave-function method to systematically investigate the binding energy and the spatial Kondo screening cloud. The variational method has been used to study the ground state of the Kondo problem in normal metals [43,44], antiferromagnets [45], 2D helical metals [46], and various novel topological materials [42,47–50]. The paper is organized as follows. We present the model Hamiltonian, dispersion, and the electron and hole pockets at the Fermi level in Sec. II. In Sec. III, we apply the variational method to study the binding energy and present the differences caused by the tilting terms. In Sec. IV, we calculate the spin-spin correlation between the magnetic impurity and the conduction electrons in a type-II WSM on three principal planes in coordinate space and analyze the results. Finally, the discussion and conclusions are given in Sec. V.

## II. THE HAMILTONIAN

We use the Anderson impurity model to study the Kondo screening of a spin-1/2 magnetic impurity in a type-II WSM; the total Hamiltonian is given by

$$H = H_0 + H_d + H_V. \tag{1}$$

$H_0$ is the kinetic energy term, $H_d$ describes the magnetic impurity part, and $H_V$ is the hybridization between the local impurity and the conduction electrons. The low-energy effective Hamiltonian of a type-II WSM in momentum space is given by

$$H_0 = \sum_{\mathbf{k}} \Psi_{\mathbf{k}}^{\dagger}[h_0(\mathbf{k}) - \mu]\Psi_{\mathbf{k}}, \tag{2}$$

with

$$\begin{aligned} h_0(\mathbf{k}) =& t'\tau_z(\sigma_x k_x + \sigma_y k_y) + t\tau_z\sigma_0 k_z + \tau_x\sigma_0 M_{\mathbf{k}} \\ &+ \lambda\tau_0\sigma_z + \left(a_{\text{tilt}}k_x + \xi k_x^2/2\right)\tau_0\sigma_0. \end{aligned} \tag{3}$$

$h_0(\mathbf{k})$ is obtained by expanding the lattice model Hamiltonian [31] (with lattice constant $a_0 = 1$), and the Fermi energy is fixed at $\mu = 0$ throughout this work. The basis vectors are given by $\Psi_{\mathbf{k}} = \{a_{\mathbf{k}\uparrow}, a_{\mathbf{k}\downarrow}, b_{\mathbf{k}\uparrow}, b_{\mathbf{k}\downarrow}\}^T$, where $a_{\mathbf{k}s}^{\dagger}$ ($b_{\mathbf{k}s}$) creates (annihilates) an electron with spin-$s$ ($s = \uparrow, \downarrow$) on the $a$ ($b$) orbit. $\sigma_\alpha$ and $\tau_\alpha$ ($\alpha = x, y, z$) are the spin and orbital Pauli matrices. $t'$ is the in-plane orbital-resolved spin-orbit coupling strength, and $t$ is the out-of-plane orbital-resolved hopping strength. In principle, $t$ and $t'$ can be different, but here we fix $t = t'$ and set them as the energy unit, in order to eliminate extra anisotropy. $M_{\mathbf{k}}$ hybridizes the two orbitals and is obtained by expanding $m_0 - t\sum_\alpha \cos k_\alpha$ around $\mathbf{k} = 0$ with $m_0 = 3t$. Notably $h_0(\mathbf{k})$ differs from the conventional type-I WSM Hamiltonian [7] by additional $a_{\text{tilt}}$ and $\xi$ terms. Moreover, in order to stop the electron and hole pockets from spreading over the entire Brillouin zone, the term $\tau_y\sigma_0 \sin k_z$ is replaced with $\tau_z\sigma_0 \sin k_z$ [31]. In the original type-I WSM Hamiltonian given in Ref. [7] in the absence of $\lambda$, $a_{\text{tilt}}$, and $\xi$, $H_0$ describes a Dirac semimetal with degenerate Dirac points located at $\mathbf{k} = 0$. A nonzero $\lambda$ breaks the time-reversal symmetry, and a type-I WSM emerges with a pair of Weyl nodes at $(0, 0, \pm\lambda/t)$ on the $k_z$ axis. The $a_{\text{tilt}}$ term tilts the Weyl cones along the $k_x$ direction, and the electron and hole pockets emerge when $a_{\text{tilt}} > \frac{(2t-m_0)^2 - t^2 + \lambda^2}{2\lambda(2t-m_0)}t'$, leading to a type-II WSM. $\xi$ further breaks the symmetry between the electron and the hole pockets around each Weyl node.

The single-particle eigenenergy is given by

$$\epsilon_{\mathbf{k}} = \pm\sqrt{\eta_{\mathbf{k}} \pm 2\nu_{\mathbf{k}}} + n_{\mathbf{k}}, \tag{4}$$

where $\nu_{\mathbf{k}} \equiv \sqrt{t^2k_z^2[\lambda^2 + t'^2(k_x^2 + k_y^2)] + \lambda^2 M_{\mathbf{k}}^2}$, $\eta_{\mathbf{k}} \equiv \lambda^2 + t'^2(k_x^2 + k_y^2) + t^2k_z^2 + M_{\mathbf{k}}^2$, and $n_{\mathbf{k}} \equiv a_{\text{tilt}}k_x + \xi k_x^2/2$. $H_0$ in its diagonal basis reads

$$H_0 = \sum_{\mathbf{k}} \Psi_{\mathbf{k}}^{\dagger} h_0(\mathbf{k})\Psi_{\mathbf{k}} = \sum_{\mathbf{k}i} \epsilon_{\mathbf{k}i}\gamma_{\mathbf{k}i}^{\dagger}\gamma_{\mathbf{k}i} \quad (i = 1, 2, 3, 4). \tag{5}$$

The relation between the eigenstates $\gamma_{\mathbf{k}i}^{\dagger}$ and $\gamma_{\mathbf{k}i}$ and the original electron creation and annihilation operators is given in the Appendix.

The localized state is described by

$$H_d = \epsilon_d \sum_{s=\uparrow,\downarrow} d_s^{\dagger}d_s + \mathrm{U}d_{\uparrow}^{\dagger}d_{\uparrow}d_{\downarrow}^{\dagger}d_{\downarrow}. \tag{6}$$

$d_s^{\dagger}$ and $d_s$ are the creation and annihilation operators of the spin-$s$ ($s = \uparrow, \downarrow$) state at the impurity site. $\epsilon_d$ is the impurity energy level, and $U$ is the on-site Coulomb repulsion.

Finally, the hybridization term between the localized state and the electron spins in the type-II WSM is given by

$$H_V = \sum_{\mathbf{k},s=\uparrow,\downarrow} V_{\mathbf{k}}[(a_{\mathbf{k}s}^{\dagger} + b_{\mathbf{k}s}^{\dagger})d_s + \text{H.c.}]. \tag{7}$$

Here $V_{\mathbf{k}} \equiv V\Theta(\Gamma - |\epsilon(\mathbf{k})|)$, where $\Theta(x)$ is a step function, which is 1 for $x > 0$ and 0 for $x < 0$. $\Gamma$ is the energy cutoff and is chosen as a large enough value so that the low-energy physics is expected to be insensitive to the value of $\Gamma$. The impurity is equally coupled to the $a$ and $b$ orbits and to the spin-up and -down states. In the diagonal basis of the type-II WSM, the hybridization part $H_V$ reads

$$H_V = \sum_{\mathbf{k}i} V_{\mathbf{k}}(\gamma_{\mathbf{k}i}^{\dagger}d_{\mathbf{k}i} + \text{H.c.}). \tag{8}$$

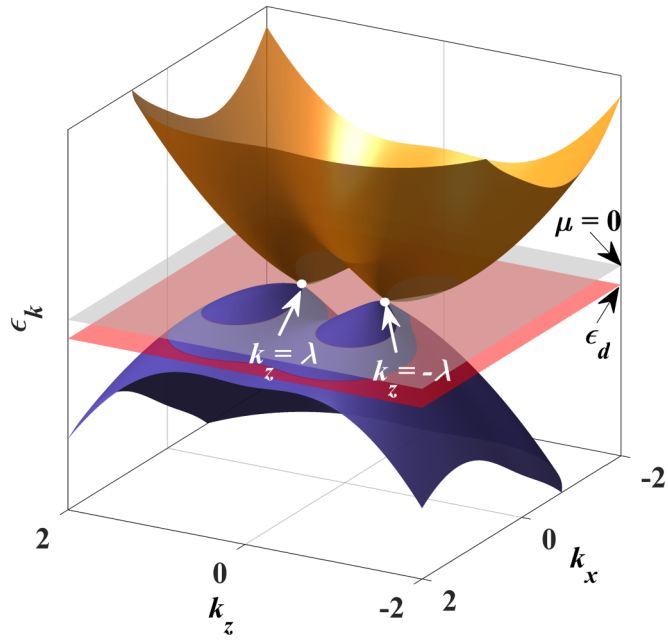


FIG. 1. Schematic of the band structure of a type-II WSM for $k_y = 0$. $\lambda$ determines the distance between the pair of Weyl nodes in a type-I WSM, $a_{\text{tilt}}$ tilts the Weyl cones along the $k_x$ axis, generating a pair of electron and hole pockets on the Fermi surface, and $\xi$ breaks the symmetry between the electron and the hole pockets. The Fermi energy is fixed at $\mu = 0$, and the energy level of the magnetic impurity is $\epsilon_d < \mu$, so for a large enough $U$ the impurity is always singly occupied.

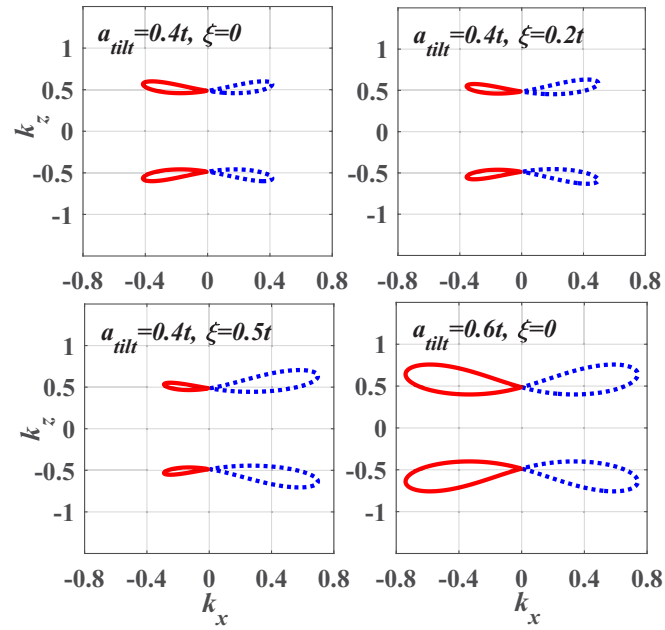


FIG. 2. Electron and hole pockets on the $k_x$-$k_z$ plane for $\lambda = 0.5t$, with different combinations of $a_{\text{tilt}}$ and $\xi$.

The $\mathbf{k}$-dependent impurity operators are connected to the original ones through the transformation

$$d^\dagger_{\mathbf{k}i} = [(\Phi_{1i} + \Phi_{3i})d^\dagger_\uparrow + (\Phi_{2i} + \Phi_{4i})d^\dagger_\downarrow] = \chi_{i1}(\mathbf{k})\, d^\dagger_\uparrow + \chi_{i2}(\mathbf{k})\, d^\dagger_\downarrow, \tag{9}$$

where $i = 1, 2, 3, 4$ are the band indices, and the definition of $\Phi_{ij}$ is given in the Appendix.

In Fig. 1 we show a schematic of the dispersion of a type-II WSM for $k_y = 0$. The two Weyl nodes are located at $k_z = \pm\lambda/t$, and the relatively large $a_{\text{tilt}}$ term generates a pair of electron and hole pockets around each Weyl node. The $\xi$ term breaks the symmetry between the electron and the hole pockets. Throughout this work, the Fermi energy is fixed at $\mu = 0$, and the magnetic impurity energy level is $\epsilon_d < \mu$. For a large enough $U$ the impurity site shall be always singly occupied.

In Fig. 2 we plot the electron and hole pockets for $\lambda = 0.5t$. The electron and hole pockets only emerge when the tilting term $a_{\text{tilt}}$ becomes large enough [31]. We can see that while $\xi = 0$, for both $a_{\text{tilt}} = 0.4t$ and $a_{\text{tilt}} = 0.6t$, the electron and hole pockets are symmetric. The finite $\xi = 0.2t$ breaks the symmetry between the pockets around each Weyl node when $a_{\text{tilt}} = 0.4t$. As $\xi$ increases, the asymmetry between the pockets becomes more significant. The tilting terms modify the DOS at the Fermi energy and also break the rotational symmetry about the $z$ axis of the type-II WSM model Hamiltonian. Hence the binding energy and the spatial Kondo screening cloud are expected to be distinct from those in a conventional type-I WSM. Notably, the essential physics remain valid even if $a_{\text{tilt}}$ and $\xi$ take a smaller magnitude.

## III. THE SELF-CONSISTENT CALCULATION

In order to investigate the eigenstate property, we utilize a trial wave-function approach. The Coulomb repulsion $U$ is assumed to be large enough, and $\epsilon_d$ is below the Fermi energy, so that the impurity site is always singly occupied by a local moment. First, we may assume that $H_V = 0$, which is the simplest case where the magnetic impurity and the host material are completely decoupled from each other. The ground state of $H_0$ is given by

$$|\Psi_0\rangle = \prod_{\mathbf{k}\in\Omega,i} \gamma_{\mathbf{k}i}{}^\dagger |0\rangle. \tag{10}$$

$i$ is the band index, and the product runs over all states within the Fermi sea $\Omega$. If we consider a singly occupied impurity and ignore the energy given by the hybridization, then the total energy of the system is just the sum of the bare impurity energy and the total energy of the WSM,

$$E_0 = \epsilon_d + \sum_{\mathbf{k}\in\Omega,i} \epsilon_{\mathbf{k}i}. \tag{11}$$

If the hybridization is taken into account and according to Eq. (8), only the conduction states and the impurity states with the same band indices are hybridized, so that the trial wave function for the ground state can be written in the diagonal basis as [46]

$$|\Psi\rangle = \left(g_0 + \sum_{\mathbf{k}\in\Omega,i} g_{\mathbf{k}i} d^\dagger_{\mathbf{k}i}\gamma_{\mathbf{k}i}\right)|\Psi_0\rangle. \tag{12}$$

$g_0$ and $g_{\mathbf{k}i}$ are all numbers and they are the variational parameters to be determined through self-consistent calculations.

The energy of the total Hamiltonian in the variational state $|\Psi\rangle$ is

$$E = \frac{\langle\Psi|H|\Psi\rangle}{\langle\Psi|\Psi\rangle}. \tag{13}$$

We can obtain $\langle\Psi|\Psi\rangle = g_0^2 + \sum_{\mathbf{k}\in\Omega,i} g_{\mathbf{k}i}^2(|\chi_{i1}(\mathbf{k})|^2 + |\chi_{i2}(\mathbf{k})|^2) = 1$ according to the wave-function normalization condition.

Then the total energy of the type-II Weyl system with a magnetic impurity in the trial state $|\Psi\rangle$ is written

$$E = \sum_{\mathbf{k}\in\Omega,i} \Big[(E_0 - \epsilon_{\mathbf{k}i} + \mu)(|\chi_{i1}(\mathbf{k})|^2 + |\chi_{i2}(\mathbf{k})|^2)g_{\mathbf{k}i}^2 + 2V_{\mathbf{k}}g_0g_{\mathbf{k}i}(|\chi_{i1}(\mathbf{k})|^2 + |\chi_{i2}(\mathbf{k})|^2) + (\epsilon_{\mathbf{k}i} - \mu)g_0^2\Big] \Big/ \left[g_0^2 + \sum_{\mathbf{k}\in\Omega,i} g_{\mathbf{k}i}^2(|\chi_{i1}(\mathbf{k})|^2 + |\chi_{i2}(\mathbf{k})|^2)\right]. \tag{14}$$

The variational principle requires that $\partial E/\partial g_0 = \partial E/\partial g_{\mathbf{k}} = 0$, leading to the two equations

$$\left(E - \sum_{\mathbf{k}\in\Omega,i} \epsilon_{\mathbf{k}i}\right) g_0 = \sum_{\mathbf{k}\in\Omega,i} V_{\mathbf{k}}g_{\mathbf{k}i}(|\chi_{i1}(\mathbf{k})|^2 + |\chi_{i2}(\mathbf{k})|^2),$$

$$(E - E_0 + \epsilon_{\mathbf{k}i})g_{\mathbf{k}i} = V_{\mathbf{k}}g_0. \tag{15}$$

We then obtain the self-consistent equation

$$\epsilon_d - \Delta_b = \sum_{\mathbf{k}\in\Omega,i} \frac{V_{\mathbf{k}}^2(|\chi_{i1}(\mathbf{k})|^2 + |\chi_{i2}(\mathbf{k})|^2)}{\epsilon_{\mathbf{k}i} - \Delta_b}, \tag{16}$$

where $\Delta_b = E_0 - E$ is the binding energy. If $\Delta_b > 0$, the hybridized state has a lower energy and is more stable than the bare state. $\Delta_b$ can be obtained by numerically solving the self-consistent equation, (16). $g_0$ and $g_{\mathbf{k}i}$ for each value of $\mathbf{k}$ and $i$ can be calculated according to the relations

$$g_0^2 + \sum_{\mathbf{k}\in\Omega,i} g_{\mathbf{k}i}^2(|\chi_{i1}(\mathbf{k})|^2 + |\chi_{i2}(\mathbf{k})|^2) = 1,$$

$$g_{\mathbf{k}i} = \frac{V_{\mathbf{k}}}{\epsilon_{\mathbf{k}i} - \Delta_b}g_0. \tag{17}$$

In Fig. 3 we present the self-consistent results of $\Delta_b$ as a function of $V_k/\Gamma$ for various combinations of $a_{\text{tilt}}$ and $\xi$. The results are obtained by numerically solving Eq. (16). Here we fix the value of $\lambda = 0.5t$, and $\Gamma$ is the energy cutoff. When $a_{\text{tilt}} = 0$ and $\xi = 0$, $H_0$ describes a type-I WSM, such that the DOS at the Fermi energy vanishes. In this case, the magnetic impurity problem falls into the category of the pseudogap Kondo problem [38–40]. The magnetic impurity and the conduction electron spins form a bound state only if the hybridization is stronger than a critical value [42]. If we slightly tilt the Weyl nodes ($a_{\text{tilt}} = 0.2t$, $\xi = 0$ or $a_{\text{tilt}} = 0$, $\xi = 0.5t$), the electron and hole pockets are not formed on the Fermi surface, so the DOS at the Fermi energy is still 0. Similarly to the case of a type-I WSM, $\Delta_b$ is positive only if $V_k$ is larger than a critical value, but the values of $\Delta_b$ slightly increase at the same hybridization strength, indicating that for the tilted system the bound state is more easily formed, although the DOS at the Fermi energy is still 0. If we go on to increase the tilting term to $a_{\text{tilt}} = 0.4t$, as shown in Fig. 2, a pair of electron and hole pockets emerges around each Weyl node, leading to a finite DOS at the Fermi energy. It is found that for $a_{\text{tilt}} = 0.4t$, $\Delta_b$ for small $V_k$ is very close to 0 but becomes a positive value. This means that for any small values of $V_k$ the impurity and the host material always form a bound state. Similar behavior has been reported in studies of magnetic impurity in a helical metal [46], topological nodal loop semimetals [50], and multi-Weyl semimetals [48]. In these systems, the DOS becomes finite if $\mu \neq 0$, and a low but positive binding energy emerges for any finite $V_{\mathbf{k}}$. If a nonzero value of $\xi$ is added, then the electron and hole pockets become asymmetric, leading to a larger DOS value at the Fermi energy. Hence for these cases the binding energy becomes higher than the symmetric case when $\xi$ is 0.

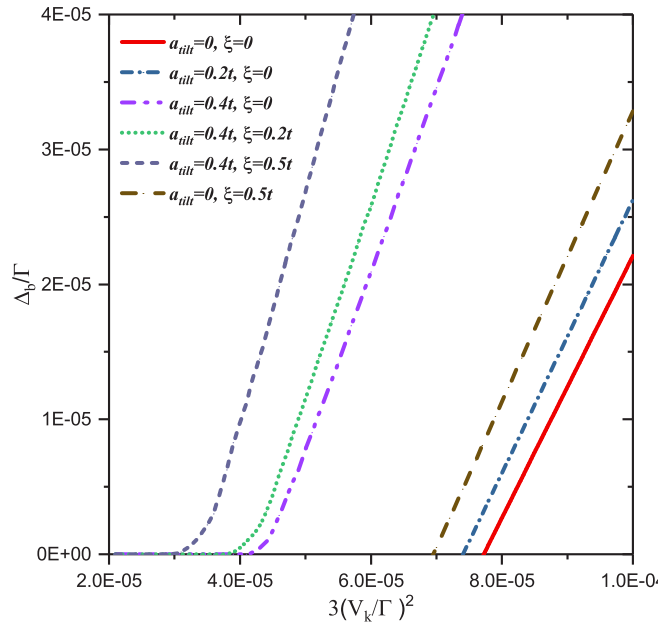


FIG. 3. Self-consistent results of the binding energy with $\lambda = 0.5t$ for various combinations of $a_{\text{tilt}}$ and $\xi$. $\mu = 0$ and $\epsilon_d = 7.5 \times 10^{-5}\Gamma$, where $\Gamma$ is the energy cutoff. There exists a critical $V_k$ to form a positive binding energy when the DOS at the Fermi energy is 0 with $\{a_{\text{tilt}} = 0, \xi = 0\}$, $\{a_{\text{tilt}} = 0.2t, \xi = 0\}$, or $\{a_{\text{tilt}} = 0, \xi = 0.5t\}$. Otherwise, when the electron and hole pockets are formed as shown in Fig. 2, the DOS becomes nonzero at the Fermi energy, so the binding energy is always positive, although the magnitude is very small when the value of $V_k$ is small.

## IV. THE SPIN-SPIN CORRELATION

In this section, we study the spin-spin correlation between the magnetic impurity and the conduction electrons in type-II WSMs. The spin operators of the magnetic impurity and conduction electrons in type-II WSMs are defined as $\mathbf{S_d} = \frac{1}{2}d^\dagger\vec{\sigma}d$, $\mathbf{S_a} = \frac{1}{2}a^\dagger\vec{\sigma}a$, and $\mathbf{S_b} = \frac{1}{2}b^\dagger\vec{\sigma}b$. $d = \{d_\uparrow, d_\downarrow\}^T$, $a = \{a_\uparrow, a_\downarrow\}^T$, and $b = \{b_\uparrow, b_\downarrow\}^T$ are the annihilation operators at the impurity site and for the two orbits in the type-II WSM, respectively. Without loss of generality, we choose the position of the magnetic impurity as $\mathbf{r} = 0$ such that the hybridization $V_k$ is in fact a constant. We also use the assumption that the

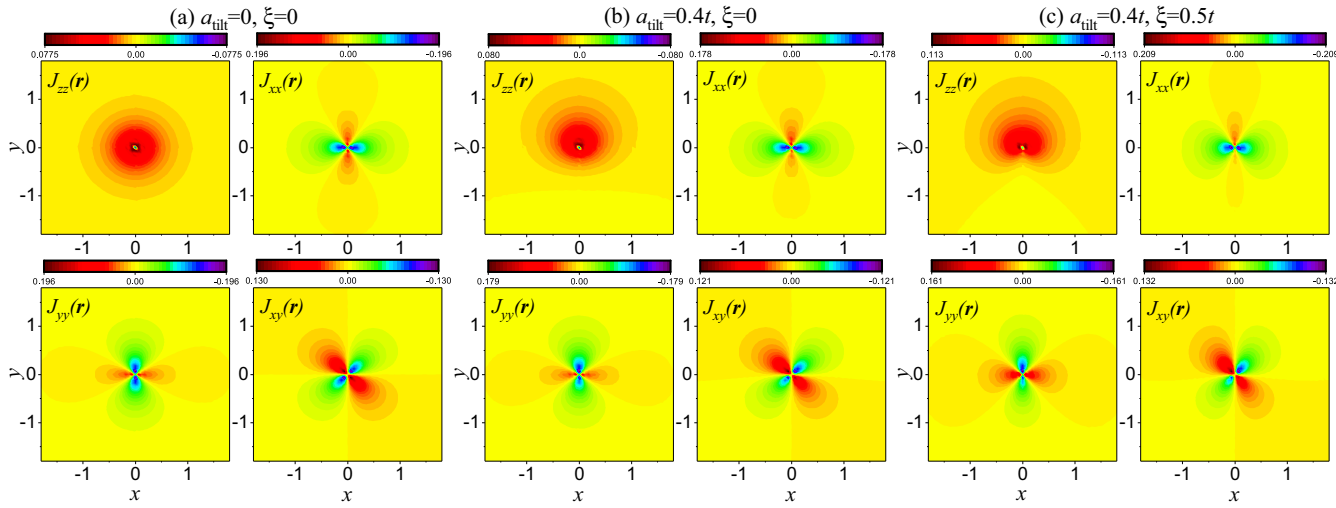


FIG. 4. Terms of the spin-spin correlation $J_{uv}$ ($u, v = x, y, z$) in the $x$-$y$ coordinate space. All the other off-diagonal terms not shown are 0 on the $x$-$y$ plane. In all the plots $\lambda = 0.5t$ and the tilting terms are (a) $a_{\rm tilt} = 0$, $\xi = 0$, (b) $a_{\rm tilt} = 0.4t$, $\xi = 0$, and (c) $a_{\rm tilt} = 0.4t$, $\xi = 0.5t$.

impurity is equally coupled to each band, such that for both the $a$ and the $b$ orbits $V_k$ is identical. Both orbits contribute to the spin-spin correlation between the magnetic impurity and the conduction electron located at $\mathbf{r}$. The correlation function consists of two parts, $J_{uv}(\mathbf{r}) = \langle S_a^u(\mathbf{r}) S_d^v(0) + S_b^u(\mathbf{r}) S_d^v(0)\rangle = J_{uv}^a(\mathbf{r}) + J_{uv}^b(\mathbf{r})$. The first term is the $a$-orbital contribution, while the second term is that of the $b$ orbital. Here $u, v = x, y, z$, and $\langle \dots \rangle$ denotes the ground-state average.

The magnitude of the binding energy $\Delta_b$ depends directly on the DOS at the Fermi energy. In a Dirac semimetal or in a type-I WSM, the DOS vanishes at the Dirac points or Weyl nodes, so there exists a threshold of the hybridization strength for a positive $\Delta_b$. However, if one tunes $\mu$ away from the Dirac points or the Weyl nodes, the DOS at the Fermi energy becomes finite. $\Delta_b$ always has a positive solution; the localized state and the conduction electrons form bound states for arbitrarily small $V_k$. On the other hand, once the bound states are formed, the spatial spin-spin correlation functions are not much affected by the choice of $\mu$ except for the magnitude. In the present paper, the spin-spin correlation function is evaluated for $\mu = 0$. The diagonal and the off-diagonal terms of the spin-spin correlation in coordinate space are given by Eq. (A5) in the Appendix. For a finite value of $\mu$, the spatial patterns of the various components of the spin-spin correlation are expected to be qualitatively the same.

In Fig. 4 to Fig. 6 we show the results of the spin-spin correlation between the local magnetic impurity and the conduction electrons on the $x$-$y$, $y$-$z$, and $x$-$z$ planes in the coordinate space. We fix $\lambda = 0.5t$, and three typical combinations of tilting terms are (i) $a_{\rm tilt} = \xi = 0$, representing a type-I WSM; (ii) $a_{\rm tilt} = 0.4t$ and $\xi = 0$, with symmetric electron and hole pockets; and (iii) $a_{\rm tilt} = 0.4t$ and $\xi = 0.5t$, representing a type-II WSM with asymmetric electron and hole pockets.

In the first case, the time-reversal symmetry is broken, but the system preserves the rotational symmetry about the $z$ axis, so we have $J_{uv}(\mathbf{r}) = J_{u'v'}(\mathbf{r}')$ if $u' = R^z(\beta)u$, $v' = R^z(\beta)v$, $\mathbf{r}' = R^z(\beta)(\mathbf{r})$, where $R^z(\beta)$ is a rotation operator about the $z$ axis. As the $a_{\rm tilt}$ and $\xi$ terms become finite the rotational symmetry about the $z$ axis is broken, but one can easily demonstrate that the Hamiltonian is still invariant under a combined operation $\mathcal{T}R^y(\pi)$, where $\mathcal{T}$ is the time-reversal operation and $R^y(\pi)$ is a rotation of angle $\pi$ about the $y$ direction. Under the transformation $\mathcal{T}R^y(\pi)$ we have

$$\begin{aligned} \{x, y, z\} &\to \{-x, y, -z\}, \\ \{k_x, k_y, k_z\} &\to \{k_x, -k_y, k_z\}, \\ \{s_x, s_y, s_z\} &\to \{s_x, -s_y, s_z\}. \end{aligned} \tag{18}$$

A large enough $a_{\rm tilt}$ generates a pair of electron and hole pockets around each Weyl node, and a nonzero $\xi$ triggers the asymmetry between the electron and the hole pockets as plotted in Fig. 2. The change in the band structure and DOS due to the $a_{\rm tilt}$ and $\xi$ terms naturally leads to the modifications in the spin-spin correlation between the magnetic impurity and the conduction electron spins. In fact, the binding energy $\Delta_b$ will take different values while the model parameters change. However, we may fix the value of $\Delta_b$ in the spin-spin correlation calculations in order to mainly concentrate on the spatial patterns. The parameters we use in this section are $V_k = 0.1t$ and $\Delta_b = 0.1t$. The length unit is chosen as $1/k_d$, where $k_d$ is the momentum cutoff. The values of $\mathcal{A}_{mn}(\mathbf{r})$ given in Eq. (A6) are complex numbers in general, so naturally the off-diagonal terms $J_{uv}(\mathbf{r}) \neq J_{vu}(\mathbf{r})$ ($u, v = x, y, z$). However, we find that $J_{uv}(\mathbf{r})$ and $J_{vu}(\mathbf{r})$ show similar patterns with the same symmetry property on the three principal planes. Hence we only plot the components $J_{xz}(\mathbf{r})$, $J_{yz}(\mathbf{r})$, and $J_{xy}(\mathbf{r})$ in the text, and others are discussed and plotted in the Appendix. A positive (negative) value of the diagonal component indicates a ferromagnetic (an antiferromagnetic) correlation between the impurity spin and the conduction electron spin.

In Fig. 4 we show the results of the diagonal and off-diagonal terms of the spin-spin correlation between the magnetic impurity and the conduction electrons on the $y$-$z$ plane in coordinate space. In Fig. 4(a) the tilting terms vanish ($a_{\rm tilt} = \xi = 0$), so the Hamiltonian describes a type-I WSM with two Weyl nodes located at $\pm\lambda/t$ on the $k_z$ axis. $\lambda$ breaks the time-reversal symmetry, but the system still preserves the rotational symmetry about the $z$ axis. Hence in Fig. 4(a) $J_{zz}(\mathbf{r})$

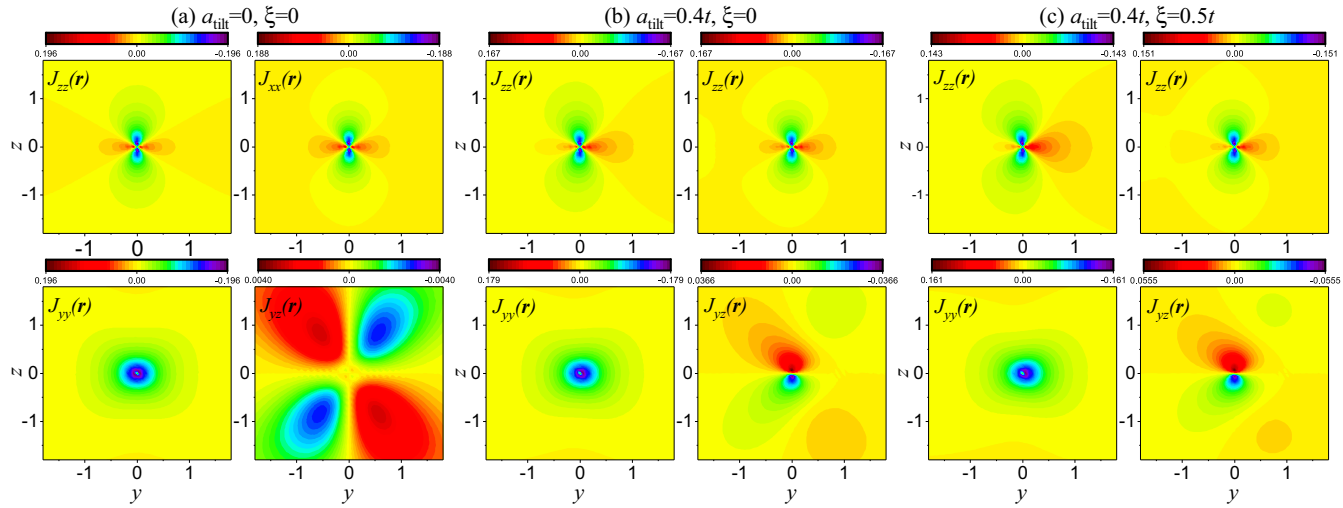


FIG. 5. Terms of the spin-spin correlation $J_{uv}$ ($u, v = x, y, z$) on the $y$-$z$ plane for $\lambda = 0.5t$. All the off-diagonal terms not shown are 0 on the $y$-$z$ plane. (a) $a_{\rm tilt} = 0$, $\xi = 0$, (b) $a_{\rm tilt} = 0.4t$, $\xi = 0$, and (c) $a_{\rm tilt} = 0.4t$, $\xi = 0.5t$.

has rotational symmetry on the $x$-$y$ plane, and the correlation is antiferromagnetic nearby the magnetic impurity and oscillates as $|\mathbf{r}|$ increases. The other two diagonal terms have the relation $J_{xx}(\mathbf{r}) = J_{yy}(R^z(\pi/2)\mathbf{r})$, and both are ferromagnetic along one real-space axis but antiferromagnetic along the other axis. Among the off-diagonal terms, only $J_{xy}(\mathbf{r})$ is nonzero. By carefully examining the results we find that the terms $J^a_{xz}(\mathbf{r}) = -J^b_{xz}(\mathbf{r})$ and $J^a_{yz}(\mathbf{r}) = -J^b_{yz}(\mathbf{r})$, so finally the off-diagonal components $J_{xz}(\mathbf{r})$ and $J_{yz}(\mathbf{r})$, vanish on the $x$-$y$ plane. According to the transformation given in Eq. (18) $J_{xy}(x, y) = -J_{xy}(-x, y)$, and if $x = 0$ the off-diagonal term $J_{xy}(\mathbf{r})$ is always 0. This is valid even if the tilting terms are added, as shown in Figs. 4(b) and 4(c), since the system is still invariant under $\mathcal{T}R^y(\pi)$. When the $a_{\rm tilt}$ term becomes finite as shown in Fig. 4(b), all four terms of the spin-spin correlation function lose the rotational symmetry of $\pi$ about the $z$ direction. We can see that all three diagonal terms are tilted along the $y$ axis, and this change is most obvious in $J_{zz}(\mathbf{r})$. The magnitude of the off-diagonal term $J_{xy}(\mathbf{r})$ also becomes asymmetric with respect to the $x$ axis. If the term $\xi$ is also imposed as shown in Fig. 4(c), the rotational symmetry is further broken. The magnitude of the spin-spin correlation shows much stronger anisotropy.

Plotted in Fig. 5 are the components of the spin-spin correlation on the $y$-$z$ principal plane. Among the off-diagonal terms, only $J_{yz}(\mathbf{r})$ is nonzero. $J_{xz}(\mathbf{r})$ and $J_{xy}(\mathbf{r})$ vanish because the $a$-orbital and $b$-orbital contributions cancel each other. In Fig. 5(a) we show the spin-spin correlation for the type-I WSM. The system preserves the rotational symmetry about the $z$ axis. Consequently, all three diagonal terms show $J_{uu}(\mathbf{r}) = J_{uu}(R^z(\pi)\mathbf{r})$ ($u = x, y, z$). Moreover, due to the $TR^y(\pi)$ symmetry, the diagonal terms also exhibit the property $J_{uu}(y, z) = J_{uu}(y, -z)$. As for the off-diagonal term we have $J_{yz}(\mathbf{r}) = J_{yz}(R^y(\pi)\mathbf{r})$ and $J_{yz}(y, z) = -J_{yz}(y, -z)$. With finite $a_{\rm tilt}$ and $\xi$ as in Figs. 5(b) and 5(c), the rotational symmetry is broken, and the WSM is only invariant under the operation $TR^y(\pi)$. In the presence of a finite $a_{\rm tilt}$ as in Fig. 5(b), we can see that the rotational symmetry of $\pi$ of spin-spin correlations is broken. However, the diagonal terms have the property $J_{zz}(y, z) = J_{zz}(y, -z)$, $J_{xx}(y, z) = J_{xx}(y, -z)$, and $J_{yy}(y, z) = J_{yy}(y, -z)$ due to the transformation given in Eq. (18). The off-diagonal term is $J_{yz}(y, z) = -J_{yz}(y, -z)$. Even if the tilting term $\xi$ is added, the system is still invariant under the combined $TR^y(\pi)$ transformation, such that diagonal terms are symmetric about the $z$ axis while the off-diagonal term is $J_{yz}(y, z) = -J_{yz}(y, -z)$.

In Fig. 6 we show the spin-spin correlation function in the $x$-$z$ coordinate space for $\lambda = 0.5t$, $a_{\rm tilt} = 0.4t$, and $\xi = 0.5t$. For the case $\lambda = 0.5t$ in the absence of tilting terms, the system has rotational symmetry about the $z$ axis and is also invariant under $TR^y(\pi)$. In this case, the results on the $x$-$z$ plane have a direct relation with those on the $y$-$z$ plane: $J_{zz}(x, z) = J_{zz}(y, z)$, $J_{xx}(x, z) = J_{yy}(y, z)$, and $J_{yy}(x, z) = J_{xx}(y, z)$. Among the off-diagonal terms, only $J_{xz}(\mathbf{r})$ is nonzero and it is related to the correlation on the $y$-$z$ plane by $J_{xz}(x, z) = J_{yz}(y, z)$. Hence when $a_{\rm tilt} = \xi = 0$, we can relate all the nonzero components of the spin-spin correlation on the $x$-$z$ plane to those on the $y$-$z$ plane.

Very interestingly, the tilting term $a_{\rm tilt} = 0.4t$ triggers nonzero off-diagonal components $J_{yz}(\mathbf{r})$ and $J_{xy}(\mathbf{r})$ on the $x$-$z$ plane. If a nonzero $\xi$ is added, the spatial pattern of the correlations are slightly modified, but the symmetry properties remain the same, so we only show the results for $\lambda = 0.5t$, $a_{\rm tilt} = 0.4t$, and $\xi = 0.5t$ in Fig. 6. Once the tilting terms become finite, the rotational symmetry about the $z$ axis is broken, but the system is still invariant under the transformation $TR^y(\pi)$. Hence the diagonal terms $J_{xx}(\mathbf{r})$, $J_{yy}(\mathbf{r})$, and $J_{zz}(\mathbf{r})$ show inversion symmetry on the $x$-$z$ plane, which can be given as $J_{uu}(x, z) = J_{uu}(-x, -z)$. The off-diagonal term $J_{xz}(\mathbf{r})$ also shows the same inversion symmetry, while $J_{yz}(\mathbf{r}) = -J_{yz}(\mathbf{r})$ and $J_{xy}(\mathbf{r}) = -J_{xy}(-\mathbf{r})$ since the spin operator $s_y \to -s_y$ under the operation $TR^y(\pi)$ as given in Eq. (18).

## V. CONCLUSIONS

In summary, we have utilized the variational wave-function method to investigate the binding energy and the spatial anisotropy of the Kondo screening cloud in a type-II WSM.

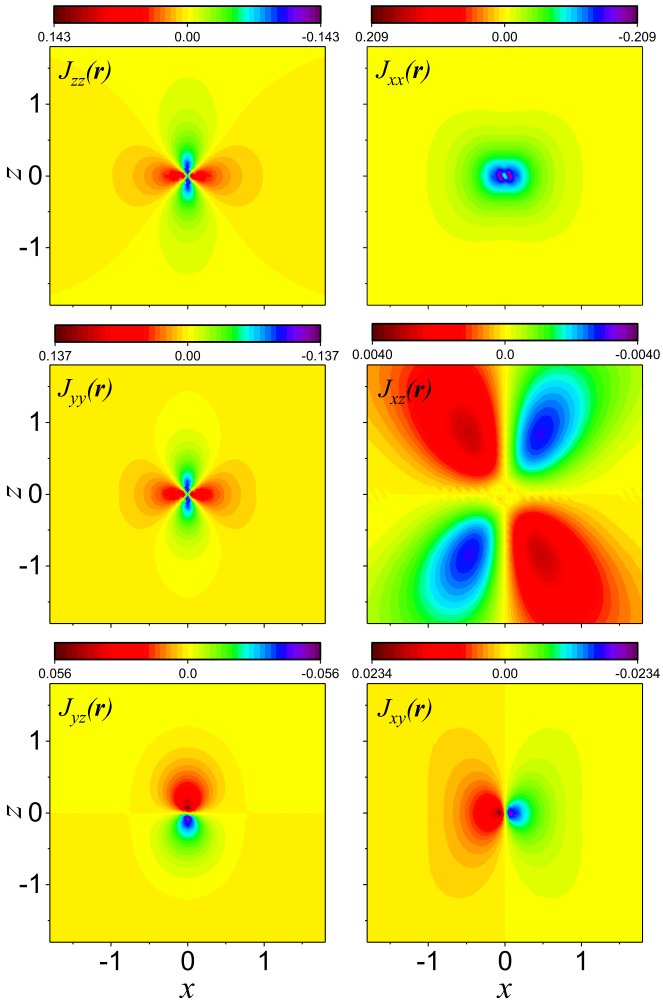


FIG. 6. Terms of the spin-spin correlation $J_{uv}(\mathbf{r})$ $(u, v = x, y, z)$ in the $x$-$z$ coordinate space for $\lambda = 0.5t$, $a_{\text{tilt}} = 0.4t$, and $\xi = 0.5t$. Due to the tilting terms the off-diagonal terms $J_{yz}(\mathbf{r})$ and $J_{xy}(\mathbf{r})$ show nonzero values on the $x$-$z$ plane.

The type-II WSM is defined by a continuous four-band model Hamiltonian, with a pair of Weyl nodes located on the $k_z$ axis. In the presence of tilting terms, the Weyl cones are tilted along the $k_x$ direction forming pairs of electron and hole pockets. The DOS becomes finite at the Fermi energy, so the Kondo effect is significantly enhanced. The bound state is always favored by the magnetic impurity and the type-II WSMs. This behavior is distinct from that of a type-I WSM, where the bound state is only formed if $V_{\mathbf{k}} > V_c$ [42], where $V_c$ is a threshold of hybridization strength. The spatial spin-spin correlation function shows very strong anisotropy due to the spin-orbit coupling and the unique band structure of the type-II system. The topology of the type-II WSM is the same as that of the type-I WSM, but the geometry of the bands and the DOS become distinct. The tilting terms $a_{\text{tilt}}$ and $\xi$ break the rotational symmetry about the $z$ direction. However, the type-II WSM model Hamiltonian remains invariant under $\mathcal{T}R^y(\pi)$. Our spin-spin correlation results reflect these changes in the host materials. All the nonzero components of the spin-spin correlation function on the three principal planes are largely modified by the tilting terms. The most significant changes are the emergence of nonzero off-diagonal correlation functions $J_{xy}(\mathbf{r})$ and $J_{yz}(\mathbf{r})$ in type-II WSMs on the $x$-$z$ coordinate plane. It has been theoretically suggested that the topology and the form of the Fermi surface of a type-II WSM are very sensitive to pressure, strain, and elastic deformation [22,51]. This offers us the opportunity to tune the Kondo effect in various regimes in the type-II WSMs. The type-II WSM also shows unique Fermi arc surface states [52], and we will address the issue of magnetic impurity in novel surface states in future work.

## ACKNOWLEDGMENTS

J.-H.S. acknowledges financial support from the NSFC (Grant No. 11604166), Zhejiang Provincial Natural Science Foundation of China (Grant No. LY19A040003), and K.C. Wong Magna Fund in Ningbo University. L.L. was supported by the NSFC (under Grant No. 11604138). D.-H.X. was supported by the NSFC (under Grant No. 11704106). W.-Q.C. acknowledges financial support from the National Key Research and Development Program of China (Grant No. 2016YFA0300300) and NSFC (Grant No. 11674151).

## APPENDIX

The $4 \times 4$ Hamiltonian of the type-II WSM $h_0(\mathbf{k})$ given in Eq. (2) can be easily diagonalized through

$$\mathcal{V}^\dagger h_0(\mathbf{k})\mathcal{V} = \mathcal{E}(\mathbf{k}). \tag{A1}$$

$\mathcal{E}(\mathbf{k})$ is the diagonal matrix whose diagonal elements are the eigenenergies. The elements of the vector matrix $\mathcal{V}$ are given by

$$\Phi_{1i} = \frac{-\lambda\left(t^2k_z^2 + M_{\mathbf{k}}^2 + q\nu_{\mathbf{k}}\right) + \left(p\nu_{\mathbf{k}} + (-1)^{i+1}tk_z\lambda\right)\sqrt{\eta_{\mathbf{k}} + 2q\nu_{\mathbf{k}}} + tk_z\left(-T^2\left(k_x^2 + k_y^2\right) - q\nu_{\mathbf{k}} - \lambda^2\right)}{T(k_x + ik_y)(\lambda - tk_z)M_{\mathbf{k}}} \cdot C_i,$$

$$\Phi_{2i} = \frac{-q\nu_{\mathbf{k}} - t^2k_z^2 + (-1)^{i+1}tk_z\sqrt{\eta_{\mathbf{k}} + 2q\nu_{\mathbf{k}}}}{(\lambda - tk_z)M_{\mathbf{k}}} \cdot C_i,$$

$$\Phi_{3i} = \frac{-q\nu_{\mathbf{k}} - \lambda^2 + (-1)^{i+1}\lambda\sqrt{\eta_{\mathbf{k}} + 2q\nu_{\mathbf{k}}}}{T(k_x + ik_y)(\lambda - tk_z)} \cdot C_i,$$

$$\Phi_{4i} = C_i. \tag{A2}$$

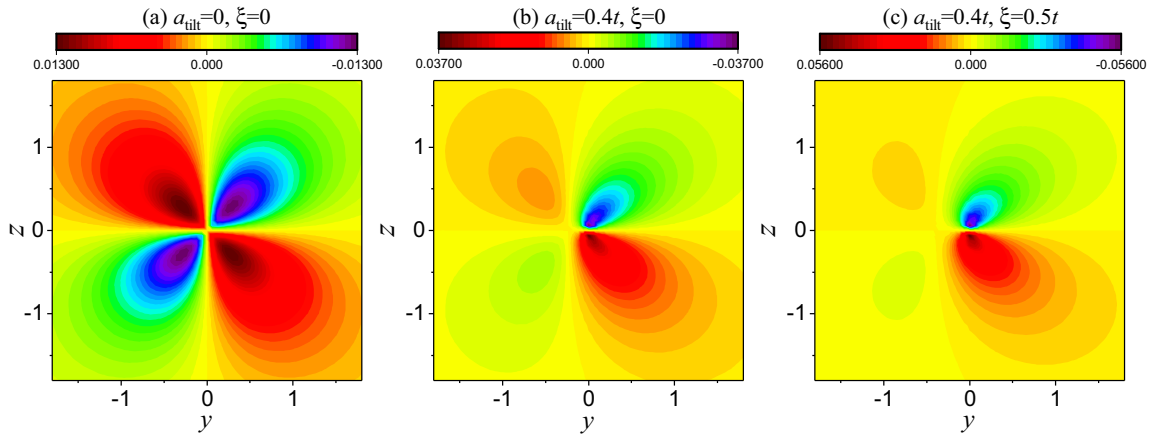


FIG. 7. $J_{zy}(\mathbf{r})$ for three combinations of $a_{\rm tilt}$ and $\xi$ on the $y$-$z$ coordinate plane for $\lambda = 0.5t$. The values are different from $J_{yz}(\mathbf{r})$ given in Fig. 5, but the symmetry property is the same.

$C_i$ $(i = 1, 2, 3, 4)$ are normalization factors, and $p$ and $q$ are simply numbers. When $i \in \{1, 2\}$, $q = -1$; otherwise, $q = +1$. When $i \in \{1, 4\}$ $p = -1$; otherwise, $p = +1$. The eigenstates of the tilted Dirac cone are given by

$$\Gamma_{\mathbf{k}} = \mathcal{V}^{\dagger}\Psi_{\mathbf{k}}, \tag{A3}$$

where $\Psi_{\mathbf{k}} = \{a_{\mathbf{k}\uparrow}, a_{\mathbf{k}\downarrow}, b_{\mathbf{k}\uparrow}, b_{\mathbf{k}\downarrow}\}^T$ and $\Gamma_{\mathbf{k}} = \{\gamma_{\mathbf{k}1}, \gamma_{\mathbf{k}2}, \gamma_{\mathbf{k}3}, \gamma_{\mathbf{k}4}\}^T$. Then $H_0$ in its diagonal basis is written

$$H_0 = \sum_{\mathbf{k}} h_0(\mathbf{k}) = \sum_{\mathbf{k}i} \epsilon_{\mathbf{k}i}\gamma^{\dagger}_{\mathbf{k}i}\gamma_{\mathbf{k}i} \quad (i = 1, 2, 3, 4). \tag{A4}$$

Both the $a$ and the $b$ orbits of the type-II WSM contribute to the spin-spin correlation between the magnetic impurity and the conduction electron located on $\mathbf{r}$. Subsequently, the correlation function consists of two parts, $J_{uv}(\mathbf{r}) = \langle S^u_a(\mathbf{r})S^v_d(0) + S^u_b(\mathbf{r})S^v_d(0)\rangle = J^a_{uv}(\mathbf{r}) + J^b_{uv}(\mathbf{r})$. Here $u, v = x, y, z$, and $\langle \dots \rangle$ denotes the ground-state average. The spin-spin correlation functions between a magnetic impurity and the conduction electrons from $a$ and $b$ orbits are given by

$$\mathbf{J}^a_{zz}(\mathbf{r}) = -\frac{1}{4}(|\mathcal{A}_{11}|^2 - |\mathcal{A}_{12}|^2 - |\mathcal{A}_{21}|^2 + |\mathcal{A}_{22}|^2),$$

$$\mathbf{J}^b_{zz}(\mathbf{r}) = -\frac{1}{4}(|\mathcal{A}_{31}|^2 - |\mathcal{A}_{32}|^2 - |\mathcal{A}_{41}|^2 + |\mathcal{A}_{42}|^2),$$

$$\mathbf{J}^a_{xx}(\mathbf{r}) = -\frac{1}{2}[\mathrm{Re}(\mathcal{A}_{12}\mathcal{A}^*_{21}) + \mathrm{Re}(\mathcal{A}_{11}\mathcal{A}^*_{22})],$$

$$\mathbf{J}^b_{xx}(\mathbf{r}) = -\frac{1}{2}[\mathrm{Re}(\mathcal{A}_{32}\mathcal{A}^*_{41}) + \mathrm{Re}(\mathcal{A}_{31}\mathcal{A}^*_{42})],$$

$$\mathbf{J}^a_{yy}(\mathbf{r}) = -\frac{1}{2}[-\mathrm{Re}(\mathcal{A}_{12}\mathcal{A}^*_{21}) + \mathrm{Re}(\mathcal{A}_{11}\mathcal{A}^*_{22})],$$

$$\mathbf{J}^b_{yy}(\mathbf{r}) = -\frac{1}{2}[-\mathrm{Re}(\mathcal{A}_{32}\mathcal{A}^*_{41}) + \mathrm{Re}(\mathcal{A}_{31}\mathcal{A}^*_{42})],$$

$$\mathbf{J}^a_{xy}(\mathbf{r}) = \frac{1}{2}[\mathrm{Im}(\mathcal{A}^*_{12}\mathcal{A}_{21}) + \mathrm{Im}(\mathcal{A}_{11}\mathcal{A}^*_{22})],$$

$$\mathbf{J}^b_{xy}(\mathbf{r}) = \frac{1}{2}[\mathrm{Im}(\mathcal{A}^*_{32}\mathcal{A}_{41}) + \mathrm{Im}(\mathcal{A}_{31}\mathcal{A}^*_{42})],$$

$$\mathbf{J}^a_{xz}(\mathbf{r}) = -\frac{1}{2}[\mathrm{Re}(\mathcal{A}_{11}\mathcal{A}^*_{21}) - \mathrm{Re}(\mathcal{A}_{12}\mathcal{A}^*_{22})],$$

$$\mathbf{J}^b_{xz}(\mathbf{r}) = -\frac{1}{2}[\mathrm{Re}(\mathcal{A}_{31}\mathcal{A}^*_{41}) - \mathrm{Re}(\mathcal{A}_{32}\mathcal{A}^*_{42})],$$

$$\mathbf{J}^a_{yz}(\mathbf{r}) = \frac{1}{2}[\mathrm{Im}(\mathcal{A}^*_{11}\mathcal{A}_{21}) + \mathrm{Im}(\mathcal{A}_{12}\mathcal{A}^*_{22})],$$

$$\mathbf{J}^b_{yz}(\mathbf{r}) = \frac{1}{2}[\mathrm{Im}(\mathcal{A}^*_{31}\mathcal{A}_{41}) + \mathrm{Im}(\mathcal{A}_{32}\mathcal{A}^*_{42})],$$

$$\mathbf{J}^a_{yx}(\mathbf{r}) = \frac{1}{2}[\mathrm{Im}(\mathcal{A}^*_{12}\mathcal{A}_{21}) - \mathrm{Im}(\mathcal{A}_{11}\mathcal{A}^*_{22})],$$

$$\mathbf{J}^b_{yx}(\mathbf{r}) = \frac{1}{2}[\mathrm{Im}(\mathcal{A}^*_{32}\mathcal{A}_{41}) - \mathrm{Im}(\mathcal{A}_{31}\mathcal{A}^*_{42})],$$

$$\mathbf{J}^a_{zx}(\mathbf{r}) = -\frac{1}{2}[\mathrm{Re}(\mathcal{A}_{12}\mathcal{A}^*_{11}) - \mathrm{Re}(\mathcal{A}_{22}\mathcal{A}^*_{21})],$$

$$\mathbf{J}^b_{zx}(\mathbf{r}) = -\frac{1}{2}[\mathrm{Re}(\mathcal{A}_{32}\mathcal{A}^*_{31}) - \mathrm{Re}(\mathcal{A}_{42}\mathcal{A}^*_{41})],$$

$$\mathbf{J}^a_{zy}(\mathbf{r}) = \frac{1}{2}[\mathrm{Im}(\mathcal{A}_{11}\mathcal{A}^*_{12}) + \mathrm{Im}(\mathcal{A}_{22}\mathcal{A}^*_{21})],$$

$$\mathbf{J}^b_{zy}(\mathbf{r}) = \frac{1}{2}[\mathrm{Im}(\mathcal{A}_{31}\mathcal{A}^*_{32}) + \mathrm{Im}(\mathcal{A}_{42}\mathcal{A}^*_{41})]. \tag{A5}$$

The function $\mathcal{A}_{mn}(\mathbf{r})$ is given by

$$\mathcal{A}_{mn}(\mathbf{r}) = \sum_{\mathbf{k}i} \Phi^*_{mi}(\mathbf{k})\chi_{in}(\mathbf{k})g_{\mathbf{k}i}e^{-i\mathbf{kr}}, \tag{A6}$$

where the numbers $\{i, j, m, n\} = \{1, 2, 3, 4\}$ are band indices. Each component of the spin-spin correlation function given in Eq. (A5) is obtained by a straightforward calculation.

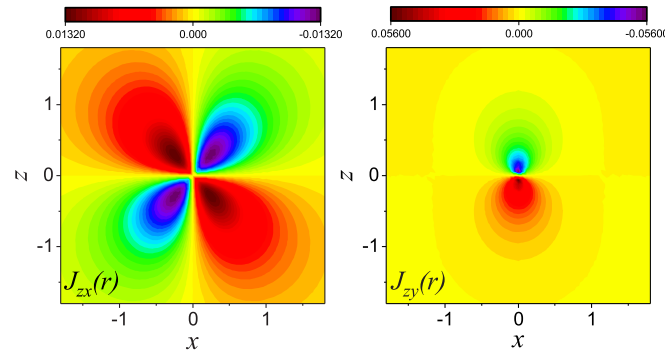


FIG. 8. $J_{zx}(\mathbf{r})$ and $J_{zy}(\mathbf{r})$ on the $x$-$z$ plane for $\lambda = 0.5t$, $a_{\rm tilt} = 0.4t$, and $\xi = 0.5t$.

To clarify, we take $J^a_{zz}(\mathbf{r})$ as an example to introduce the process. We remember the hybridized wave function in Eq. (12), and when it is normalized, the correlation function is given by

$$\begin{aligned} J^a_{zz}(\mathbf{r}) &= \langle\Psi|s^z_a(\mathbf{r})s^z_d(0)|\Psi\rangle \\ &= \langle\Psi_0|\left(g_0+\sum_{\mathbf{p}m} g_{\mathbf{p}m}\gamma^\dagger_{\mathbf{p}m}d_{\mathbf{p}m}\right)s^z_a(\mathbf{r})s^z_d(0) \\ &\quad\times\left(g_0+\sum_{\mathbf{q}n} g_{\mathbf{q}n}d^\dagger_{\mathbf{q}n}\gamma_{\mathbf{q}n}\right)|\Psi_0\rangle. \end{aligned} \tag{A7}$$

$s^z_a(\mathbf{r})$ can be transformed to the diagonal basis of conduction electrons following Eq. (A3), and we can easily know that

$$\langle\Phi_0|\gamma^\dagger_{\mathbf{p}m}\gamma^\dagger_{\mathbf{k}i}\gamma_{\mathbf{k}'j}\gamma_{\mathbf{q}n}|\Phi_0\rangle = \delta_{\mathbf{pq}}\delta_{mn}\delta_{\mathbf{kk}'}\delta_{ij} - \delta_{\mathbf{pk}'}\delta_{mj}\delta_{\mathbf{kq}}\delta_{in}. \tag{A8}$$

The first term in Eq. (A8) returns $\mathbf{r}$-independent results, and only the second term, which shows the spatial patterns, is of interest to us. The spatial spin-spin correlation function is then given by

$$\begin{aligned} J^a_{zz}(\mathbf{r}) &= \frac{1}{4}\sum_{\mathbf{k}\mathbf{k}'ij}(\Phi^*_{1i}(\mathbf{k})\Phi_{1j}(\mathbf{k}') - \Phi^*_{2i}(\mathbf{k})\Phi'_{2j}(\mathbf{k}'))e^{-i(\mathbf{k}-\mathbf{k}')\mathbf{r}}\langle\Psi_0|g_{\mathbf{k}i}g_{\mathbf{k}'j}d_{\mathbf{k}'j}(d^\dagger_\uparrow d_\uparrow - d^\dagger_\downarrow d_\downarrow)d^\dagger_{\mathbf{k}i}|\Psi_0\rangle \\ &= \frac{1}{4}\sum_{\mathbf{k}\mathbf{k}'ij}(\Phi^*_{1i}(\mathbf{k})\Phi_{1j}(\mathbf{k}') - \Phi^*_{2i}(\mathbf{k})\Phi'_{2j}(\mathbf{k}'))e^{-i(\mathbf{k}-\mathbf{k}')\mathbf{r}}g_{\mathbf{k}i}g_{\mathbf{k}'j}(\chi^*_{j1}(\mathbf{k}')\chi_{i1}(\mathbf{k}) - \chi^*_{j2}(\mathbf{k}')\chi_{i2}(\mathbf{k})) \\ &= -\frac{1}{4}(|\mathcal{A}_{11}(\mathbf{r})|^2 - |\mathcal{A}_{12}(\mathbf{r})|^2 - |\mathcal{A}_{21}(\mathbf{r})|^2 + |\mathcal{A}_{22}(\mathbf{r})|^2). \end{aligned} \tag{A9}$$

Other components of the spin-spin correlation function can be obtained in similar ways.

$\mathcal{A}_{mn}(\mathbf{r})$ values given in Eq. (A6) are complex numbers, so $J_{uv}(\mathbf{r}) \neq J_{vu}(\mathbf{r})$ in general. Below we mainly analyze the nonzero off-diagonal components of the spin-spin correlation on the three principal planes.

$J_{xy}(\mathbf{r})$ and $J_{yx}(\mathbf{r})$ are nonzero on the $x$-$y$ plane and, also, on the $x$-$z$ plane in the presence of tilting terms. We find that the second terms of $J^a_{xy}(\mathbf{r})$ and $J^b_{xy}(\mathbf{r})$ cancel each other, meaning that $\mathrm{Im}(\mathcal{A}_{11}\mathcal{A}^*_{22}) + \mathrm{Im}(\mathcal{A}_{31}\mathcal{A}^*_{42}) = 0$. Consequently, on the $x$-$y$ and $x$-$z$ coordinate planes, $J_{xy}(\mathbf{r}) = J_{yx}(\mathbf{r})$.

$J_{yz}(\mathbf{r})$ and $J_{zy}(\mathbf{r})$ are nonzero on the $y$-$z$ plane and, also, on the $x$-$z$ plane in the presence of tilting terms. On the $y$-$z$ plane, $J_{yz}(\mathbf{r}) \neq J_{zy}(\mathbf{r})$, and we plot the results of $J_{zy}(\mathbf{r})$ on the $y$-$z$ plane in Fig. 7.

On the $x$-$z$ plane, and in the absence of $a_{\mathrm{tilt}}$ and $\xi$, the model Hamiltonian of the type-II WSM preserves the rotational symmetry about the $z$ direction. Hence one may have $J_{xz}(x,z) = J_{yz}(y,z)$ and $J_{zx}(x,z) = J_{zy}(y,z)$. In Fig. 8 we show the results for nonzero off-diagonal components of the spin-spin correlation function on the $x$-$z$ plane. Remarkably, we find that $J_{zy}(\mathbf{r})$ is negative when $z > 0$, while $J_{yz}(\mathbf{r})$ is positive. The values of $J_{zx}(\mathbf{r})$ are different in comparison to those of $J_{xz}(\mathbf{r})$ plotted in Fig. 6.


[1] N. P. Armitage, E. J. Mele, and A. Vishwanath, Rev. Mod. Phys. **90**, 015001 (2018).

[2] Z. Liu, B. Zhou, Y. Zhang, Z. Wang, H. Weng, D. Prabhakaran, S.-K. Mo, Z. Shen, Z. Fang, X. Dai *et al.*, Science **343**, 864 (2014).

[3] Z. Liu, J. Jiang, B. Zhou, Z. Wang, Y. Zhang, H. Weng, D. Prabhakaran, S.-K. Mo, H. Peng, P. Dudin, T. Kim, M. Hoesch, Z. Fang, X. Dai, Z. Shen, D. Feng, Z. Hussain, and Y. Chen, Nat. Mater. **13**, 677 (2014).

[4] M. Neupane, S.-Y. Xu, R. Sankar, N. Alidoust, G. Bian, C. Liu, I. Belopolski, T.-R. Chang, H.-T. Jeng, H. Lin *et al.*, Nat. Commun. **5**, 3786 (2014).

[5] X. Wan, A. M. Turner, A. Vishwanath, and S. Y. Savrasov, Phys. Rev. B **83**, 205101 (2011).

[6] A. A. Burkov, M. D. Hook, and L. Balents, Phys. Rev. B **84**, 235126 (2011).

[7] M. M. Vazifeh and M. Franz, Phys. Rev. Lett. **111**, 027201 (2013).

[8] H. Weng, C. Fang, Z. Fang, B. A. Bernevig, and X. Dai, Phys. Rev. X **5**, 011029 (2015).

[9] S.-M. Huang, S.-Y. Xu, I. Belopolski, C.-C. Lee, G. Chang, B. Wang, N. Alidoust, G. Bian, M. Neupane, C. Zhang, S. Jia, A. Bansil, H. Lin, and M. Hasan, Nat. Commun. **6**, 7373 (2015).

[10] S.-Y. Xu, I. Belopolski, N. Alidoust, M. Neupane, G. Bian, C. Zhang, R. Sankar, G. Chang, Z. Yuan, C.-C. Lee, S.-M. Huang, H. Zheng, J. Ma, D. Sanchez, B. Wang, A. Bansil, F. Chou, P. Shibayev, H. Lin, S. Jia, and M. Hasan, Science **349**, 613 (2015).

[11] B. Q. Lv, H. M. Weng, B. B. Fu, X. P. Wang, H. Miao, J. Ma, P. Richard, X. C. Huang, L. X. Zhao, G. F. Chen, Z. Fang, X. Dai, T. Qian, and H. Ding, Phys. Rev. X **5**, 031013 (2015).

[12] S.-Y. Xu, N. Alidoust, I. Belopolski, Z. Yuan, G. Bian, T.-R. Chang, H. Zheng, V. Strocov, D. Sanchez, G. Chang, C. Zhang, D. Mou, Y. Wu, L. Huang, C.-C. Lee, S.-M. Huang, B. Wang, A. Bansil, H.-T. Jeng, T. Neupert, A. Kaminski, H. Lin, S. Jia, and M. Zahid Hasan, Nat. Phys. **11**, 748 (2015).

[13] C.-L. Zhang, Z. Yuan, Q.-D. Jiang, B. Tong, C. Zhang, X. C. Xie, and S. Jia, Phys. Rev. B **95**, 085202 (2017).

[14] L. Yang, Z. Liu, Y. Sun, H. Peng, H. Yang, T. Zhang, B. Zhou, Y. Zhang, Y. Guo, M. Rahn, D. Prabhakaran, Z. Hussain, S.-K. Mo, C. Felser, B. Yan, and Y. Chen, Nat. Phys. **11**, 728 (2015).

[15] Z. Wang, Y. Zheng, Z. Shen, Y. Lu, H. Fang, F. Sheng, Y. Zhou, X. Yang, Y. Li, C. Feng, and Z.-A. Xu, Phys. Rev. B **93**, 121112(R) (2016).
[16] X. Huang, L. Zhao, Y. Long, P. Wang, D. Chen, Z. Yang, H. Liang, M. Xue, H. Weng, Z. Fang, X. Dai, and G. Chen, Phys. Rev. X **5**, 031023 (2015).
[17] B. Lv, N. Xu, H. Weng, J. Ma, P. Richard, X. Huang, L. Zhao, G. Chen, C. Matt, F. Bisti, V. Strocov, J. Mesot, Z. Fang, X. Dai, T. Qian, M. Shi, and H. Ding, Nat. Phys. **11**, 724 (2015).
[18] A. Lopez-Bezanilla and P. B. Littlewood, Phys. Rev. B **93**, 241405(R) (2016).
[19] M. O. Goerbig, J.-N. Fuchs, G. Montambaux, and F. Piéchon, Phys. Rev. B **78**, 045415 (2008).
[20] M. Hirata, K. Ishikawa, G. Matsuno, A. Kobayashi, K. Miyagawa, M. Tamura, C. Berthier, and K. Kanoda, Science **358**, 1403 (2017).
[21] A. A. Soluyanov, Physics **10**, 74 (2017).
[22] A. A. Soluyanov, D. Gresch, Z. Wang, Q. Wu, M. Troyer, X. Dai, and B. A. Bernevig, Nature (London) **527**, 495 (2015).
[23] Y. Xu, F. Zhang, and C. Zhang, Phys. Rev. Lett. **115**, 265304 (2015).
[24] Y. Sun, S.-C. Wu, M. N. Ali, C. Felser, and B. Yan, Phys. Rev. B **92**, 161107 (2015).
[25] Z. Wang, D. Gresch, A. A. Soluyanov, W. Xie, S. Kushwaha, X. Dai, M. Troyer, R. J. Cava, and B. A. Bernevig, Phys. Rev. Lett. **117**, 056805(R) (2016).
[26] K. Deng, G. Wan, P. Deng, K. Zhang, S. Ding, E. Wang, M. Yan, H. Huang, H. Zhang, Z. Xu *et al.*, Nat. Phys. **12**, 1105 (2016).
[27] L. Huang, T. M. McCormick, M. Ochi, Z. Zhao, M.-T. Suzuki, R. Arita, Y. Wu, D. Mou, H. Cao, J. Yan *et al.*, Nat. Mater. **15**, 1155 (2016).
[28] J. Jiang, Z. Liu, Y. Sun, H. Yang, C. Rajamathi, Y. Qi, L. Yang, C. Chen, H. Peng, C. Hwang *et al.*, Nat. Commun. **8**, 13973 (2017).
[29] G. Chang, S.-Y. Xu, D. S. Sanchez, S.-M. Huang, C.-C. Lee, T.-R. Chang, G. Bian, H. Zheng, I. Belopolski, N. Alidoust *et al.*, Sci. Adv. **2**, e1600295 (2016).
[30] S.-Y. Xu *et al.*, Sci. Adv. **3**(6), e1603266 (2017).
[31] T. E. O'Brien, M. Diez, and C. W. J. Beenakker, Phys. Rev. Lett. **116**, 236401 (2016).
[32] Z.-M. Yu, Y. Yao, and S. A. Yang, Phys. Rev. Lett. **117**, 077202 (2016).
[33] S. Tchoumakov, M. Civelli, and M. O. Goerbig, Phys. Rev. Lett. **117**, 086402 (2016).
[34] M. Udagawa and E. J. Bergholtz, Phys. Rev. Lett. **117**, 086401 (2016).
[35] Y. Ferreiros, A. A. Zyuzin, and J. H. Bardarson, Phys. Rev. B **96**, 115202 (2017).
[36] S. Saha and S. Tewari, Eur. Phys. J. B **91**, 4 (2018).
[37] J. Kondo, Prog. Theor. Phys. **32**, 37 (1964).
[38] C. Gonzalez-Buxton and K. Ingersent, Phys. Rev. B **57**, 14254 (1998).
[39] L. Fritz and M. Vojta, Phys. Rev. B **70**, 214427 (2004).
[40] M. Vojta and L. Fritz, Phys. Rev. B **70**, 094502 (2004).
[41] L. Li, J.-H. Sun, Z.-H. Wang, D.-H. Xu, H.-G. Luo, and W.-Q. Chen, Phys. Rev. B **98**, 075110 (2018).
[42] J.-H. Sun, D.-H. Xu, F.-C. Zhang, and Y. Zhou, Phys. Rev. B **92**, 195124 (2015).
[43] O. Gunnarsson and K. Schönhammer, Phys. Rev. Lett. **50**, 604 (1983).
[44] C. M. Varma and Y. Yafet, Phys. Rev. B **13**, 2950 (1976).
[45] V. Aji, C. M. Varma, and I. Vekhter, Phys. Rev. B **77**, 224426 (2008).
[46] X.-Y. Feng, W.-Q. Chen, J.-H. Gao, Q.-H. Wang, and F.-C. Zhang, Phys. Rev. B **81**, 235411 (2010).
[47] D. Ma, H. Chen, H. Liu, and X. C. Xie, Phys. Rev. B **97**, 045148 (2018).
[48] H.-F. Lü, Y.-H. Deng, S.-S. Ke, Y. Guo, and H.-W. Zhang, Phys. Rev. B **99**, 115109 (2019).
[49] J.-H. Sun, L.-J. Wang, X.-T. Hu, L. Li, and D.-H. Xu, Phys. Rev. B **97**, 035130 (2018).
[50] Y.-H. Deng, H.-F. Lü, S.-S. Ke, Y. Guo, and H.-W. Zhang, J. Phys.: Condens. Matter **30**, 435602 (2018).
[51] M. Zubkov and M. Lewkowicz, Ann. Phys. **399**, 26 (2018).
[52] H. Zheng and M. Z. Hasan, Adv. Phys.: X **3**, 1466661 (2018).